Digest Journal of Nanomaterials and Biostructures Vol. 12, No. 2, April - June 2017, p. 235 - 242

SYNTHESIS OF NICKEL-COPPER NANOCRYSTALLINE FERRITE ADSORBENTS FOR TREATMENT OF TEXTILE EFFLUENTS

A. S. KHAN[a,b], A. GHAFFAR[b], M. Y. NAZ[b*], M. AZAM[b], Y. KHAN[c], I. AHMAD[c]

[a]*Department of Material Science and Engineering, Shandong University, Jinan 250061, China*

[b]*Department of Physics, University of Agriculture, 38040 Faisalabad, Pakistan*

[c]*Department of Electrical Engineering, King Saud University, Riyadh, Saudi Arabia*

This study investigated the potential of nano-crystalline nickel-copper ferrites as an absorbent material for treatment of waste water effluent of dye industry. Co-precipitation technique was employed to synthesize the different concentrations of nickel-copper ferrite absorbent from hexa-hydrated copper chloride, hexa-hydrated nickel chloride and hexa-hydrated ferric chloride with NaOH as a digesting agent. The concentration effect on crystal structure, crystal size, volume of the unit cell, density of the unit cell, lattice parameters and microstructures of the produced spinel ferrites was elaborated using X-ray diffraction (XRD) analysis and scanning electron microscope (SEM). The crystalline cubic structures of $Ni_{0.9}Cu_{0.1}Fe_2O_4$, $Ni_{0.7}Cu_{0.3}Fe_2O_4$ and $Ni_{0.5}Cu_{0.5}Fe_2O_4$ phases were formed after 2 hours of annealing at 700^{o}C and using NaOH as precipitating agent. The waste water from dye industry was analyzed using UV–VIS spectrophotometry before and after treating with these nano-crystalline ferrites. The highest degree of dye separation from the waste water effluent was achieved with solid to liquid ratio of 0.3:50. It was revealed that all the ferrite samples showed highest dye removal efficiency during the first 60 min of stirring.

(Received November 23, 2016; Accepted April 3, 2017)

Keywords: Dye industry; waste water; nanocrystalline ferrites, dye absorbents.

1. Introduction

The most important element on earth and essential for vital activities of living beings is water (Pearce, et al. 2003). Unfortunately, the quality of our water is continuously declining due to the geometric population growth, industrialization and agricultural activities, and other geological changes. Therefore pollution of water has become a serious problem in the current scenario, disturbing all living creatures, recreation, housekeeping, fishing, transportation and other business activities (Seckler, et al. 1999). Over the last few decades, thousands of inorganic and organic pollutants have been reported as water impurities. Many of them are poisonous and have shown serious side effects; some being deadly and hazardous. These pollutants are showing drastic effects on the human health, water conditions, and the ecosystem of the earth as a whole (Ali 2012).

The dyes, pigments and other similar kind of materials are essentially used in textile, plastic, paper, food, leather and cosmetic for coloring the product. The release of colored waste water from such industries may pose threats to the environment. This colorful waste affects the operation of aquatic photosynthesis, reduces the oxygen content in the water, and in severe cases, leads to suffocation of aquatic plants and animals (Cooper 1993). The dyes like Congo red must be removed from the industrial waste discharged to the streams, otherwise it can reduce light penetration into the waste and consequently the photosynthesis of sewage receiving stream (Wang, et al. 2012). Even in very low concentrations, heavy metals and contaminants in the waste water

*Corresponding Author: yasin306@uaf.edu.pk

may cause heavier exposure to some of the living organisms and the environment. Heavy metals such as nickel, copper and zinc may appear to human toxicity and carcinogenicity therefore should be dealt carefully (Mishra and Patel 2009) .

Methylene blue (MB), Congo red (CR) and basic fuchsine (BF) are examples of cationic dye structure widely used as dyes. Various methods, such as adsorption, advanced oxidation, coagulation and membrane separation are being used to remove the dyes from the waste water. Adsorption is the most advanced and effective waste water treatment process and industrial application (Yagub, et al. 2014). Many absorbent products have been studied for the discoloration of waste water (Hanafi, et al. 2010). Numerous studies report the use of magnetic ferrite nanoparticles, produced by various methods, for the treatment of chemically polluted water due to their low cost, larger surface area and high recovery, exceptional magnetic properties and reuse (Vîrlan, et al. 2013).

Magnetic nano-crystalline ferrites having a large specific surface area and small diffusion resistance provide a separation mechanism where the particles with an affinity to target species are mixed with the heterogeneous solution. Upon mixing with the solution, the particles tag the target species. The external magnetic fields are then applied to separate the tagged particles from the solution (Afkhami, et al. 2010). This study was aimed at investigating the potential of nano-crystalline nickel-copper ferrites as an absorbent material for treatment of waste water effluent of dye industry. Co-precipitation technique was employed to synthesize the different concentrations of nickel-copper ferrite absorbent from hexa-hydrated copper chloride, hexa-hydrated nickel chloride and hexa-hydrated ferric chloride with NaOH as a digesting agent. The crystalline cubic structures of $Ni_{0.9}Cu_{0.1}Fe_2O_4$, $Ni_{0.7}Cu_{0.3}Fe_2O_4$ and $Ni_{0.5}Cu_{0.5}Fe_2O_4$ phases were formed using NaOH as precipitating agent. The waste water from dye industry was treated with the as prepared ferrites and analyzed using UV–VIS spectrophotometry before and after treatment.

2. Materials and methods

The AR grade chemicals including hexa hydrated nickel chloride ($NiCl_2.6H_2O$), hexa hydrated copper chloride ($CuCl_2.6H_2O$), hexa hydrated ferric chloride ($FeCl_3.6H_2O$), sodium hydroxide (NaOH) and acetone (CH_3COCH_5) were imported from Sigma-Aldrich (Germany). All the chemicals and reagents, used in the conducted research work were of high purity. To obtain the desired ferrite composition, stoichiometric amounts of $NiCl_2.6H_2O$ (nickel chloride hexa hydrated), $CuCl_2$ (copper chloride), $FeCl_3.6H_2O$ (Ferric chloride hexa hydrated) salts were dissolved in distilled water and subjected to the magnetic stirring. The precipitant agent (NaOH) was used to attain the desired pH of 12 (Calvin, et al. 2010). The sodium hydroxide also accelerated the reaction and limited the formation of other phases. The possible reaction can be expressed using the equation:

$$(1-x)NiCl_2.6H_2O + xCuCl_2 + 2FeCl_3.6H_2O + NaOH \rightarrow Ni_{1-x}Cu_xFe_2O_4 + NaCl + H_2O \quad (1)$$

where x=0.1,0.3,0.5

The composition of $Ni_{1-x}Cu_xFe_2O_4$ was selected as: $x = 0.1, 0.3, 0.5$, for all three samples. The beaker containing the dark brown precipitates was placed into pre-heated water bath containing water. The temperature of water bath was kept constant at 90^{o}C for preparation of the samples. After 90 min of heating under continuous stirring, the precipitates were settled down at the bottom of the beaker. The precipitates were filtered and washed thoroughly with distilled water to make them free from sodium and chloride ions. The final product was dried in an electric oven at heating temperature of 60^{o}C for 4 hours to remove the moisture contents. The fully dried samples were grinded to obtain the desired particle size. Before grinding the samples, pestle and mortar were washed carefully with acetone (CH_3COCH_5). Thereafter, the grinded precursor was annealed at 700^{o}C for 2 h. The annealed samples were set to cool slowly under ambient temperature condition.

The spontaneous magnetization of ferrite particles was checked using permanent magnets. The ferrite phases were identified through X-ray diffraction (XRD) analysis and the morphology of the prepared ferrites was examined using scanning electron microscope (SEM). Particle size in the ferrite samples was determined using Scherrer's formula (Rohadiana, et al. 2011). In the later stage, the fully characterized ferrite powders were used as an adsorbent material for dye removal from the waste water effluent of the dye industry. The waste water, before and after dye removal, was analyzed using UV–VIS spectrophotometry. The spectra were recorded in the range of 400–800 nm. In order to determine the efficiency of the studied adsorbent, the influence of the solid-liquid (S:L) ratio and contact time on the removal efficiency was studied. To identify the optimum S:L ratio, 50 mL of residual water was treated with various quantities of adsorbent material (0.1, 0.2 and 0.3 g). The water-ferrite mixture was shaken for 1 hour using an overhead magnetic stirrer at moderate speed of 300 rpm. After dye absorption, the absorbent was separated from the treated water through magnetic filtration. The resulting solution was analyzed again using UV-visible spectrophotometry. Once the optimum S:L ratio was established, the influence of stirring time (15, 30, 45, 60, 75, 90, 105 and 120 min) on adsorption capacity of the ferrite absorbent was investigate. The degree of adsorption of nickel copper ferrites was calculated using the following equation (Ali 2012):

$$\text{Adsorption Efficiency } (\eta) = \frac{Initial\ Adsorption - Final\ Adsorption}{Initial\ Adsorption} \times 100 \quad (2)$$

where η represents the removal degree of dye.

3. Results and discussion

3.1. XRD Analysis

XRD patterns of $Ni_{1-x}Cu_xFe_2O_4$ powders, prepared using co-precipitation method, are shown in Fig. 1. The shown patterns confirm the formation of ferrite phases in the identified crystalline structures. The diffraction peaks also confirmed the good crystallization of the product (Liu, et al. 2013). Sharp diffraction peaks, consistent with face centered cubic spinel structure, were noticed in XRD patterns of all the investigated samples. Peaks at 2θ of 30.55^o, 35.98^o, 37.52^o, 43.58^o, 57.66^o and 63.32^o were referred to XRD diffraction planes (220), (311), (222), (400), (333) and (440), respectively. These peaks confirmed the formation of cubic spinel nickel copper ferrite when compared with JCPDS card 070-2674. The crystal size of $Ni_{1-x}Cu_xFe_2O_4$ ferrite samples was determined by considering the most intense diffraction peaks (311) in XRD patterns. In this study, the Debye-Scherrer formula was used to calculate the crystal size of tested samples:

$$T = 0.9\ \lambda/\beta Cos\theta \quad (3)$$

Where 'θ' is the Bragg angle between incident ray and diffracted plane, 'λ' is the wavelength of X-rays used and 'β' is measured in radians (line broadening at intensity equal to the half maximum intensity). The Debye-Scherrer formula gives rough estimate of the crystalline size of the material, based on the width of XRD peaks (Cullity 1978). Table 1 shows the average crystalline size of the samples having different concentrations. It can be noticed that the values of the crystal size for S-1 (coprecipitated $Ni_{0.9}Cu_{0.1}Fe_2O_4$), S-2 (coprecipitated $Ni_{0.7}Cu_{0.3}Fe_2O_4$) and S-3 (coprecipitated $Ni_{0.5}Cu_{0.5}Fe_2O_4$) annealed at same temperature of 700^oC, are 23.21 nm, 32.05 nm and 30.93 nm, respectively. It is also observed that the crystal size decreases with a decrease in the concentration of $Ni_{1-x}Cu_xFe_2O_4$ and increases with an increase in the ferrite concentration. The average crystal size decreases with the decreasing Ni content in $Ni_{1-x}Cu_xFe_2O_4$ nanoparticles. It may be due to small grain growth of Ni (Mote *et al.*, 2013). It was also seen that the crystal size increases with an increase in annealing temperatures (Shinde, et al. 2008).

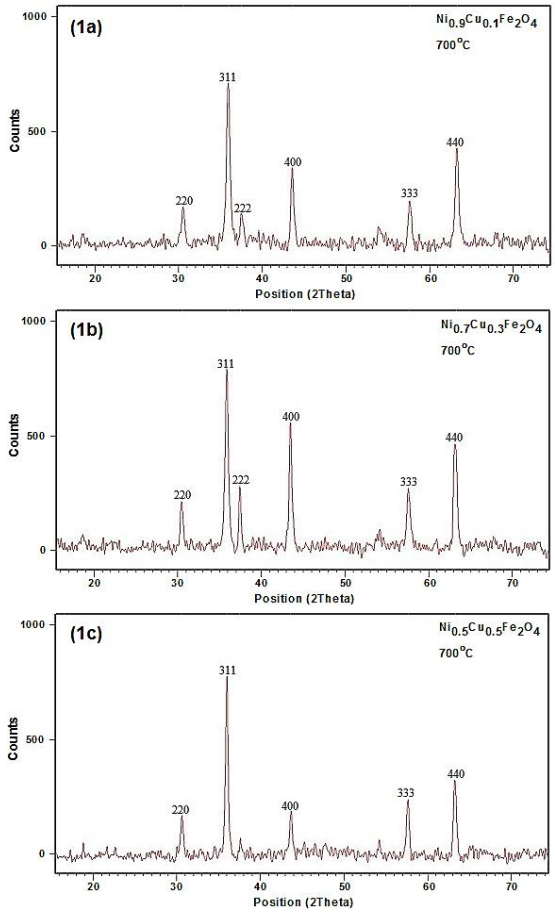

Fig. 1. XRD patterns of co-precipitated (1a) $Ni_{0.9}Cu_{0.1}Fe_2O_4$ ferrite, (1b) $Ni_{0.7}Cu_{0.3}Fe_2O_4$ ferrite, and (1c) $Ni_{0.5}Cu_{0.5}Fe_2O_4$ ferrite

Table 1. Crystal size of $Ni_{1-x}Cu_xFe_2O_4$ ferrites

Code	$[M^+/OH^-]$	Temperature (^oC)	Crystalline size (nm)
S-1	0.1	700	23.21
S-2	0.3	700	32.05
S-3	0.5	700	30.93

The lattice constant of $Ni_{1-x}Cu_xFe_2O_4$ ferrites was calculated using the d-values, obtained from Fig. 1, in the following relation (Wahab, 2005):

$$d = a / (h^2 + k^2 + l^2)^{1/2} \quad (4)$$

The lattice constant calculated for the cubic spinel structures is given in Table 2. It is observed that the values of lattice constant for S-1, S-2 and S-3 are 8.3 Å, 8.31 Å and 8.29 Å, respectively. Lattice constant of $Ni_{1-x}Cu_xFe_2O_4$ was not significantly influenced by a change in concentration. Negligible effect of different concentrations on the lattice constant was noted in the presented work. For all the samples, the lattice constant values were in a close agreement with the results published by the American Society for Testing Materials (Joseyphus, et al. 2006).

Table 2. Lattice constant of $Ni_{1-x}Cu_xFe_2O_4$ ferrites

Code	$[M^+/OH^-]$	Temperature (^oC)	Lattice constant (Å)
S-1	0.1	700	8.3
S-2	0.3	700	8.31
S-3	0.5	700	8.29

The volume of the unit cell of the synthesized samples was calculated using the respective lattice constant values from Table 2. The relation between the volume and the lattice constant exists in the form:

$$V = a^3 \tag{5}$$

The calculated volume of the samples is given in Table 3. It can be seen that the values of volume of the unit cell for S-1, S-2 and S-3 are 571.06 $Å^3$, 574.64 $Å^3$ and 570.73 $Å^3$, respectively. Negligible effect of concentration on volume of the unit cell of $Ni_{1-x}Cu_xFe_2O_4$ was seen due to negligible variation in lattice constants.

Table 3. Volume of unit cell of $Ni_{1-x}Cu_xFe_2O_4$ ferrites

Code	Temperature (^oC)	[M+/OH-]	Volume ($Å^3$)
S-1	700	0.1	571.06
S-2	700	0.3	574.64
S-3	700	0.5	570.73

X-Ray density of the ferrite samples was determined using the formula:

$$D = 8M / Na^3 \tag{6}$$

Where 'M' is the molecular weight of the $Ni_{1-x}Cu_xFe_2O_4$, which is different for each sample due to different concentrations. Its value for S-1, S-2 and S-3 samples is 234.8687, 235.8392 and 236.8097, respectively. 'N' is the Avogadro's No. and 'a' is the lattice constant of the sample (Gul *et al*. 2008). The calculated values of X-ray density for different samples are given in Table 4. It is observed that the value of X-ray density for S-1, S-2 and S-3 samples is 5.47 g/cm^3, 5.45 g/cm^3 and 5.52 g/cm^3, respectively.

Table 4. Density of $Ni_{1-x}Cu_xFe_2O_4$ ferrites at 700^oC

Code	Mol. Weight	[M+/OH-]	Density (g/cm^3)
S-1	234.8687	0.1	5.47
S-2	235.8392	0.3	5.45
S-3	236.8097	0.5	5.52

3.2. SEM Analysis

Scanning electron microscopy was carried out to understand the morphology of the synthesized material. The SEM micrographs in Fig. 2 reveal similar morphology of nanoparticles of different compositions. The particle size of the samples was found is in the nanometer regime with narrow size distribution. The grains were homogenously distributed. In SEM analysis, the sample having concentration of 0.1, the particle size was measured about 23.21 nm, which was

same as calculated from Sherrer's formula in XRD analysis. Similarly, the sample having the concentration of 0.5 the particle size was measured about 30.21 nm.

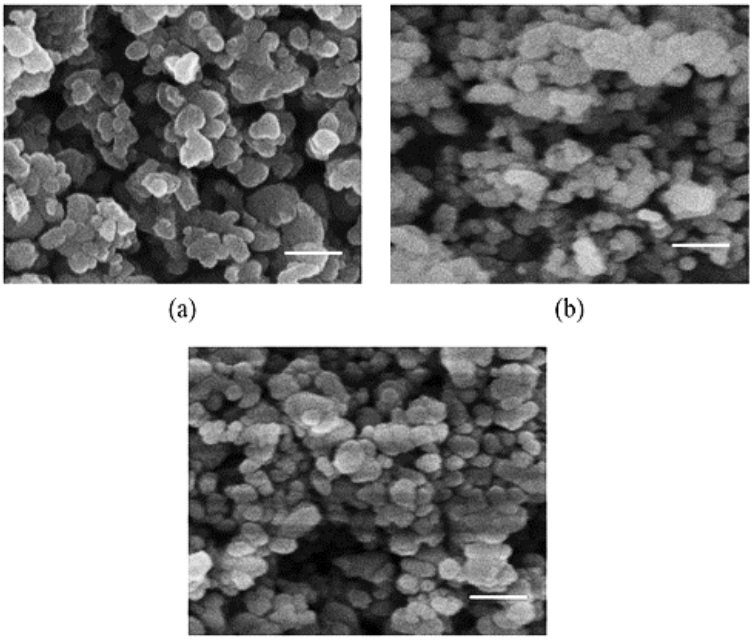

Fig. 2. SEM images of calcined samples: (a) S-1, (b) S-2, and (c) S-3 with scale bar of 2 mμ.

3.3. Waste Water Treatment

The obtained ferrites were used for the treatment of waste water resulted from dye industry. The used waste water effluent of dye industry was analyzed through UV–VIS spectrophotometry. Fig. 3 shows the UV–VIS spectra of the waste water before and after treatment with the ferrite. The studied waste water contained different colors at different specific wavelengths. As the waste water showed maximum absorption at 532 nm wavelength, which reflects high proportion of dye in the analyzed water. Therefore, in subsequent studies, this wavelength was used to obtain absorption values. Fig. 3 shows that the adsorption efficiency of coprecipitated $Ni_{1-x}Cu_xFe_2O_4$ is 84%. The influence of the S:L ratio on the adsorption efficiency of the studied ferrites is presented in the Table 5. It can be observed that the adsorption efficiency of S-1 is 51.41, S-2 is 49.61 and S-3 is 54.96. S-3 had the maximum adsorption efficiency with S:L ration of 0.3:50.

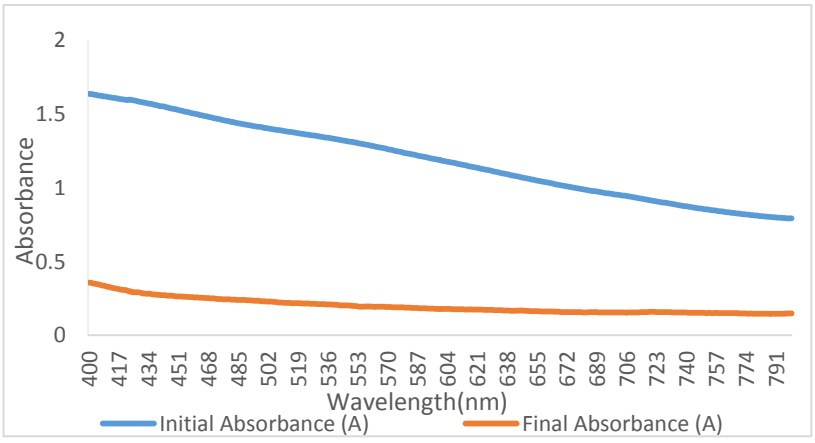

Fig. 3. UV–VIS spectra of the waste water before and after treatment.

Table 5: The influence of S:L ration on the adsorption efficiency of ferrites.

Sample code	S:L Ratio	Adsorption efficiency (%)
S-1	0.1:50	51.41
S-2	0.2:50	49.61
S-3	0.3:50	54.96

From the experimental data, it can be observed that the use of a higher quantity of $Ni_{1-x}Cu_xFe_2O_4$ did not lead to more separation of dye from the waste water. The variations of adsorption efficiency of coprecipitated $Ni_{0.9}Cu_{0.1}Fe_2O_4$, $Ni_{0.7}Cu_{0.5}Fe_2O_4$ and $Ni_{0.5}Cu_{0.5}Fe_2O_4$ ferrites with respect to stirring time are shown in the Table 6. It can also be observed that for all three samples, the highest removal efficiency of the dye from waste waters is obtained in the first 60 min of stirring. At higher stirring times, the adsorption efficiency did not increase significantly, therefore it is not recommended to employ higher stirring times from the economic point of view. Also, it can be noticed from the following Table 6 that the S-1 and S-3 present a higher efficiency as compared with the S-2. This could be explained by the fact that the particle size of the S-1 and S-3 was smaller than S-2, therefore the surface contact between the adsorbent and adsorbate was higher (Voda, et al. 2015).

Table 6: A influence of stirring time on the adsorption efficiency ferrites.

Stirring time	Adsorption efficiency (%)		
(min)	S-1	S-1	S-1
15	42.81	43.77	49.27
30	50.84	47.64	51.21
45	50.99	47.79	52.70
60	51.14	48.01	57.23
75	51.28	50.61	57.23
90	52.40	51.65	57.31
105	55.23	52.03	57.38
120	56.56	55.37	57.38

4. Conclusions

Nickel-copper ferrite nanoparticles have been successfully synthesized using chemical co-precipitation technique. The well single cubic structures of $Ni_{0.9}Cu_{0.1}Fe_2O_4$, $Ni_{0.7}Cu_{0.3}Fe_2O_4$ and $Ni_{0.5}Cu_{0.5}Fe_2O_4$ phases were formed after annealing al 700^{o}C for 2h using NaOH as precipitating agent. The XRD patterns of co-precipitated and digested samples showed the (3 1 1) peak at 2θ=35. With an increase in concentration of $Ni_{1-x}Cu_xFe_2O_4$ ferrite, the the crystal size was also increased. The average crystal size for all the three samples of $Ni_{1-x}Cu_xFe_2O_4$ was remained in the range of 23.21 nm to 30.93 nm.

The range of lattice constant for all the three samples are 8.3Å, 8.31Å and 8.29Å. The highest degree of separation of the dye from the waste water effluent of dye industry was obtained with S:L ratio of 0.1g : 50ml at stirring time of 120 min. It was observed that for all three samples, the highest removal efficiency of the dye from the waste water was possible during the first 60 min of stirring. At higher stirring times, the adsorption efficiency was not significantly by the time.

Acknowledgments

Authors would like to extend their sincere appreciation to the Deanship of Scientific Research at King Saud University for funding this work through Research Group No. RG1438-012.

References

[1] Afkhami Abbas, Mohammad Saber-Tehrani, Hasan Bagheri, Desalination **263**(1), 240 (2010).
[2] Ali Imran, Chemical reviews **112**(10), 5073 (2012).
[3] S. Calvin, et al. Journal of applied physics **107**(2), 024301 (2010).
[4] P. Cooper, Journal of the Society of Dyers and Colourists **109**(3), 97 (1993).
[5] B. D. Cullity, Elements of X-ray Diffraction, 2nd. Adisson-Wesley Publis hing. USA. 1978.
[6] F. Hanafi, O. Assobhei, M. Mountadar, Journal of Hazardous Materials **174**(1),807 (2010).
[7] Joseyphus, R Justin, et al., Journal of Physics and Chemistry of Solids **67**(7), 1510 (2006).
[8] Y. Liu, et al., Physics Procedia **50**, 43 (2013).
[9] P. C. Mishra, R. K. Patel, Journal of Hazardous Materials **168**(1), 319 (2009).
[10] C. I. Pearce, J. R. Lloyd, J. T. Guthrie, Dyes and pigments **58**(3), 179 (2003).
[11] D. N. Rohadiana, et al., Journal of Materials Science & Technology **27**(11), 991 (2011).
[12] Seckler, David, Randolph Barker, Upali Amarasinghe, International Journal of Water Resources Development **15**(1-2), 29 (1999).
[13] T. J. Shinde, A. B. Gadkari, P. N. Vasambekar, Materials Chemistry and Physics **111**(1), 87 (2008).
[14] Vîrlan, Constantin, et al., Acta Chemica Iasi **21**(1), 19 (2013).
[15] RalucaVoda, et al., Open Chemistry **13**(1), (2015).
[16] Wang, Lixia, et al., Chemical Engineering Journal **181**, 72 (2012).
[17] Yagub, Mustafa T, et al., Advances in colloid and interface science **209**, 172 (2014).